

## Phosphorus speciation changes across the glass transition in highly polymerized alkali silicate glasses and melts

BJORN MYSÉN\*

Geophysical Laboratory, 5251 Broad Branch Road, NW, Washington, D.C. 20015, U.S.A.

### ABSTRACT

In situ, high-temperature Raman spectroscopy of  $\text{Na}_2\text{O}\cdot 9\text{SiO}_2$  glasses and melts with and without 2 mol%  $\text{P}_2\text{O}_5$  has been conducted to 1491 K (near the liquidus temperature). In the temperature range from 298 to  $\sim 1000$  K (below the glass-transition temperature range), orthophosphate ( $\text{PO}_4^{3-}$ ) complexes appear to be the dominant phosphate species present. As temperature increases above  $\sim 1000$  K, the orthophosphate complex is partially replaced by pyrophosphate complexes ( $\text{P}_2\text{O}_7^{4-}$ ) so that at  $\sim 1200$  K  $>70\%$  of the P exists in the latter form. The proportion of pyrophosphate species does not change significantly as the temperature further increases. This change in phosphate speciation is accompanied by an increase in the  $\text{Q}^3/\text{Q}^4$  silicate species abundance ratio. At the highest temperatures there is also evidence for  $\text{Q}^2$  species in the melts.

The transformation from orthophosphate to pyrophosphate implies depolymerization of the silicate network because the P/O ratio in the  $\text{P}_2\text{O}_7^{4-}$  complex is smaller than in  $\text{PO}_4^{3-}$ . This depolymerization is consistent with the change in  $\text{Q}^3/\text{Q}^4$  ratio in the silicate. Therefore, use of P speciation data from glasses would lead to overestimation of the degree of polymerization of P-bearing silicate melts.

### INTRODUCTION

The geochemical behavior of P in natural magmatic systems is receiving increasing attention (e.g., Harrison and Watson 1984; Pichavant et al. 1992; Toplis et al. 1994; Wolf and London 1994). Although generally present in comparatively low concentrations in natural magmas (<2–3 wt%  $\text{P}_2\text{O}_5$ ), P strongly modifies both the physical and chemical properties of silicate liquids (e.g., Wyllie and Tuttle 1964; Kushiro 1975; Watson 1976; Ryerson and Hess 1980; London 1987; Toplis et al. 1994).

Results of in situ examination of silicate melt and glass structures at high temperature indicate that above the glass transition there is a gradual change in the proportion of the silicate structural units (Q species) with increasing temperature. The enthalpy of the relevant speciation reactions typically is on the order of 10–40 kJ/mol (e.g., Stebbins et al. 1992; McMillan et al. 1992; Mysen and Frantz 1992, 1993). These studies also indicate that the structure of silicate glasses reflects the structure frozen in at the glass-transition temperature. Glass structure cannot be used, therefore, for quantitative description of silicate liquids. To characterize the structural role of P in silicate melts at high temperature, in situ, high-temperature studies similar to those conducted for silicate speciation in melts is needed. This is the purpose of the present study.

Results from structural studies of glass indicate poten-

tially complex interactions between P, alkali and alkaline earths, Al, Si, and Fe (e.g., Mysen et al. 1981; Nelson and Tallant 1984; Dupree et al. 1988; Gan and Hess 1992; Mysen 1992). In light of this complexity, a database for the structural behavior of P in silicate melts at high temperature is needed. Choosing a simple silica-rich composition ( $\text{Na}_2\text{O}\cdot 9\text{SiO}_2$ ) with fixed P content (~2 mol%  $\text{P}_2\text{O}_5$ ) was the first step in this process. This composition provides a simple model for the role of alkali-silicate interaction in a melt that has a degree of polymerization (NBO/Si = 0.1) that is similar to that found in felsic magmatic liquids (granite and rhyolite).

### EXPERIMENTAL METHODS

The starting material was prepared (denoted NS9) by heating a thoroughly mixed  $\text{Na}_2\text{CO}_3 + \text{SiO}_2$  oxide to 1600 °C for about 1 h. The melt was then quenched to a glass. P was added as ammonium dihydrogen phosphate ( $\text{NH}_4\text{H}_2\text{PO}_4$ ) in a proportion appropriate to yield NS9 + 2 mol%  $\text{P}_2\text{O}_5$  in the final glass starting material. The glass +  $\text{NH}_4\text{H}_2\text{PO}_4$  mixture was ground for 1 h under alcohol and transformed to an  $\text{NH}_4^+$ ,  $\text{H}_2\text{O}$ ,  $\text{PO}_4^{3-}$ -containing glass by subjecting this mixture, contained in sealed platinum containers, to 1700 °C at 10 kbar for 1 h in a solid-media, high-pressure apparatus. This procedure was employed to avoid volatilization of the P which would occur if the glass +  $\text{NH}_4\text{H}_2\text{PO}_4$  mixture was subjected to the required temperatures in open sample containers. The temperature was then decreased to 1550 °C at 1 atm for ~30 min to remove the ammonium and  $\text{H}_2\text{O}$  from the high-pressure

\* Member of NSF-sponsored Center for High Pressure Research (CHiPR).

**TABLE 1.** Composition of starting materials (wt%)

Oxide	NS9	NS9 + 2 mol% P <sub>2</sub> O <sub>5</sub>
SiO <sub>2</sub>	90.24	88.44
Al <sub>2</sub> O <sub>3</sub>	0.02	0.21
Na <sub>2</sub> O	9.42	9.05
P <sub>2</sub> O <sub>5</sub>	—	3.95
Total	99.68	101.65

glass. The glass was checked for homogeneity and analyzed with a JEOL 8900 electron microprobe (Table 1). Also shown is the analyzed composition of the P-free base glass.

About 1 mg glass chips from the starting material were used for the high-temperature, in situ structural work, which was conducted with confocal, microRaman spectroscopy using the heating system described by Mysen and Frantz (1993). The sample was optically examined continuously during the high-temperature experiments with the petrographic microscopic attached to the Raman spectrometer (625× magnification). This was done to ascertain that there was no bubble formation, phase separation, or crystal nucleation while the high-temperature Raman spectra were acquired.

About 500 mW of the 514 nm line from an Ar<sup>+</sup> ion argon laser was used for sample excitation. Raman spectra were recorded with an EG&G Model 4000 CCD with acquisition times ranging from 30 to 60 s per CCD window. Two windows were needed to collect the spectra in the frequency range of first-order Raman scattering from these samples. The experiments were conducted by first recording a glass spectrum at 25 °C followed by the spectrum at the highest temperatures and then recording the

spectra at successively lower temperatures and finishing with another spectrum at 25 °C. The process was then reversed by heating the same sample with the same temperature steps until the highest temperature was reached.

The high-frequency portion of the spectra (700–1300 cm<sup>-1</sup>) was curve fitted with the method described by Mysen (1992, 1996) to determine the appropriate number of lines, the line shape, and the line parameters for each band. All line parameters and the fraction of Gaussian component were determined by minimizing the  $\chi^2$  and maximizing the residual distribution using the algorithm by Davidon (1966).

The glass cannot be physically removed from the heater after chemical analysis without destruction of the heater. Instead, to evaluate whether compositional degradation of the sample occurred during the high-temperature experimental series, the initial and final glass spectra were compared. By calibrating the changes in Raman spectra of glasses along the join Na<sub>2</sub>O-SiO<sub>2</sub>, Mysen (1995) found that spectral changes reflecting  $\pm 1$  wt% change in Na<sub>2</sub>O content could be detected with this method.

## RESULTS AND DISCUSSION

The 298 K spectrum of NS9 glass (Fig. 1A) is similar to that reported by Mysen et al. (1982). With increasing temperature, most spectral features broaden, as do those of other alkali silicate melts at similar temperatures.

By dissolving ~2 mol% P<sub>2</sub>O<sub>5</sub> in the glass, a strong, narrow peak near 940 cm<sup>-1</sup> dominates the spectrum (Fig. 1B). In comparison with the P-free glass (Fig. 1A), other spectroscopic changes are subtle. With increasing temperature the band near 940 cm<sup>-1</sup> becomes less intense,

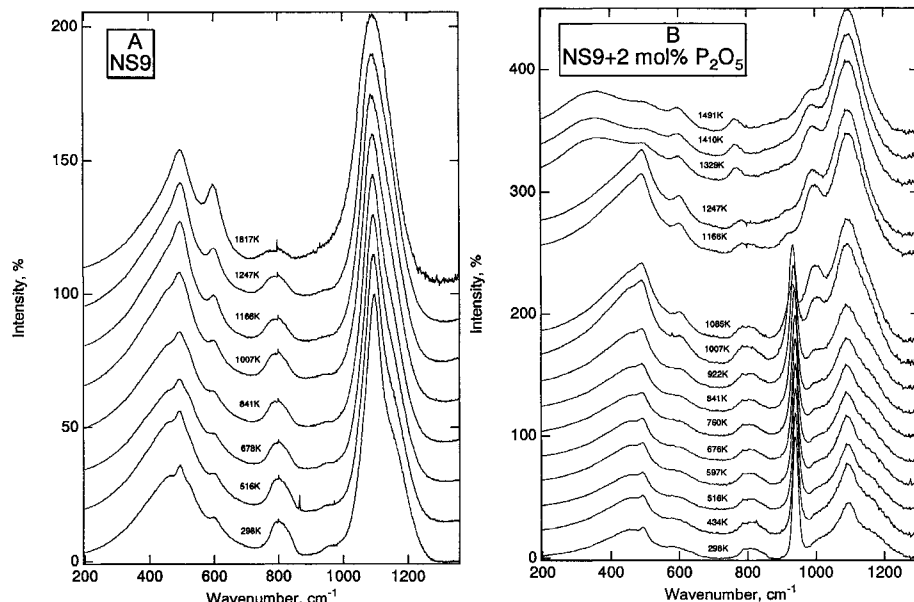


**FIGURE 1.** Unpolarized Raman spectra as a function of temperature (as indicated on individual spectra) for NS9 composition and NS9 + 2 mol% P<sub>2</sub>O<sub>5</sub>.

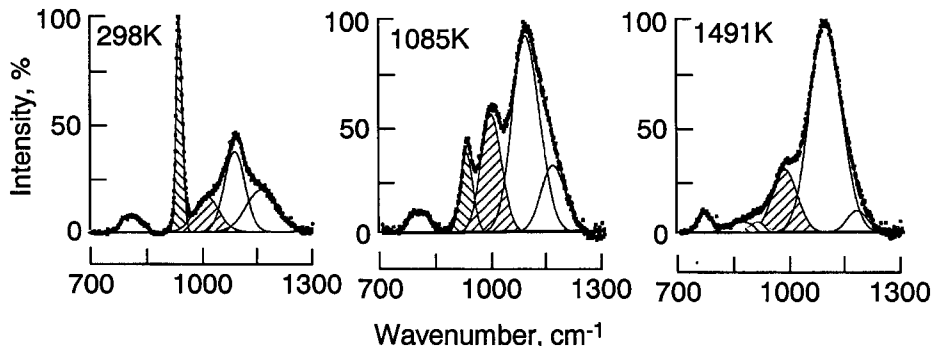


**FIGURE 2.** Examples of curve-fitted Raman spectra in the 700–1300  $\text{cm}^{-1}$  frequency range at temperatures indicated. Hatched bands are those assigned to P-O<sup>-</sup> stretching in  $\text{PO}_4^{3-}$  and  $\text{P}_2\text{O}_7^{4-}$  complexes.

and a new band grows near 1000  $\text{cm}^{-1}$ . This effect becomes particularly evident as the temperature exceeds 900 K. The 940  $\text{cm}^{-1}$  band decays to a barely visible shoulder at  $T > 1247$  K, whereas the band near 1000  $\text{cm}^{-1}$  remains strong. Above 1247 K additional spectral changes occur in the low-frequency region, with the peak centered near 500  $\text{cm}^{-1}$  in the lower temperature spectra becoming much broader and less distinct, coupled with the development of a broad intensity maximum centered near 400  $\text{cm}^{-1}$  (Fig. 1B). The broad band slightly above 800  $\text{cm}^{-1}$  becomes sharper and is shifted to about 780  $\text{cm}^{-1}$ . These spectroscopic changes are reversible across the temperature range examined.

To obtain more detailed information, the frequency range between 700 and 1300  $\text{cm}^{-1}$  was fitted to five or six Gaussian lines (six lines were required for spectra taken at  $T > 1200$  K). This frequency range includes those bands that can be assigned to Si-O<sup>-</sup> and P-O<sup>-</sup> stretching vibrations in species with different degrees of polymerization (different NBO/Si and NBO/P ratios). Three examples (298 K glass, a supercooled liquid at 1085 K, and liquid at 1491 K) are shown in Figure 2. The strongest band, near 1100  $\text{cm}^{-1}$ , is assigned to Si-O<sup>-</sup> stretching in  $\text{Q}^3$  structural units, and that near 1150  $\text{cm}^{-1}$  to Si-O<sup>0</sup> stretching in  $\text{Q}^4$  units. The weak band near 870  $\text{cm}^{-1}$  in spectra taken at  $T > 1200$  K is tentatively assigned to Si-O<sup>-</sup> stretching in silicate species less polymerized than  $\text{Q}^3$ . This species is here referred to as  $\text{Q}^2$ , but this assignment remains uncertain. The broad band near 800  $\text{cm}^{-1}$  in the low-temperature spectra is present whether or not P is present (Fig. 1). The band is assigned to an in-cage O motion in fully polymerized structural units,  $\text{Q}^4$  (e.g., McMillan et al. 1992; Mysen 1995). The bands near 940 and 1000  $\text{cm}^{-1}$  are assigned to P-O<sup>-</sup> stretching in ortho-( $\text{PO}_4^{3-}$ ) and pyrophosphate ( $\text{P}_2\text{O}_7^{4-}$ ), respectively (shaded in Fig. 2), consistent with  ${}^3\text{P}$  NMR and Raman spectroscopy of other P-bearing alkali and alkaline earth silicate glasses (Nelson and Tallant 1984; Dupree et al. 1988; Gan and Hess 1992; Mysen 1992). In silicate glasses in which the pyrophosphate complexes dominate, the presence of  $\text{P}_2\text{O}_7^{4-}$  is also associated with increased Raman intensity near 400  $\text{cm}^{-1}$  and a distinct

peak near 780  $\text{cm}^{-1}$  (Nelson and Tallant 1984). Those spectroscopic features (broad 400  $\text{cm}^{-1}$  band and sharp 780  $\text{cm}^{-1}$  band) resemble the present spectra in the high-temperature range where the 1000  $\text{cm}^{-1}$  band dominates over that near 940  $\text{cm}^{-1}$ . It is concluded, therefore, that the spectroscopic changes at high temperature are due to vibrations associated with the greatly increased abundance of  $\text{P}_2\text{O}_7^{4-}$  species in the melts in comparison with the lower temperature glasses.

The integrated intensity ratio (area) of the 940  $\text{cm}^{-1}$  ( $\text{PO}_4^{3-}$ ) and 1000  $\text{cm}^{-1}$  ( $\text{P}_2\text{O}_7^{4-}$ ) bands and of the 1100  $\text{cm}^{-1}$  ( $\text{Q}^3$ ) and 1150  $\text{cm}^{-1}$  ( $\text{Q}^4$ ) bands as a function of temperature is shown in Figure 3. At temperatures below ~1000 K, the area ratio,  $A_{940}/A_{1000}$ , may show a gradual decrease, although within the error of the data this decrease might be questionable. Between ~1000 and 1200 K this ratio decreases by >85%, followed by a very slow decrease at even higher temperature (Fig. 3A). The  $A_{1100}/A_{1150}$  ratio displays the opposite temperature dependence with a rapid increase in the 1000–1200 K temperature interval (Fig. 3B).

The liquidus temperature for the composition NS9 + 2 mol%  $\text{P}_2\text{O}_5$  is about 1470 K [on the basis of the liquidus temperature of pure NS9 (Kracek 1930) adjusted for solution of 2 mol%  $\text{P}_2\text{O}_5$  under the assumption of ideal mixing in the melt]. From the empirical relationship,  $T_g = \frac{1}{2}T_{liq}$ , this liquidus temperature,  $T_{liq}$ , yields a temperature for the onset of the glass transition,  $T_g$ , of 980 K. It would appear, therefore, that the rapid change in the integrated intensity ratios,  $A_{940}/A_{1000}$  and  $A_{1100}/A_{1150}$ , corresponds to the

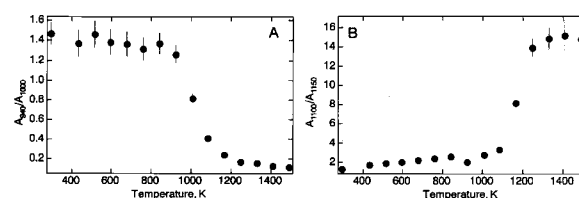


**FIGURE 3.** Area ratio of the 940 to 1000  $\text{cm}^{-1}$  bands,  $A_{940}/A_{1000}$  (A), and of the 1100 and 1150  $\text{cm}^{-1}$  bands,  $A_{1100}/A_{1150}$  (B), as a function of temperature.

temperature at which  $\text{NS9} + 2 \text{ mol\% P}_2\text{O}_5$  is transformed from a glass containing P mostly in the form of orthophosphate species,  $\text{PO}_4^{3-}$ , to a supercooled liquid in which P occurs primarily as pyrophosphate units,  $\text{P}_2\text{O}_7^{4-}$ . By assuming that the  $A_{940}/A_{1100}$  ratio is proportional to the concentration ratio of the two phosphate species in the glass and melt, the mole fraction of  $\text{P}_2\text{O}_7^{4-}$  increases from ~0.4 to ~0.9 across the glass-transition temperature range. This assumption is justified because the 940 and 1000  $\text{cm}^{-1}$  bands both are assigned to  $\text{P}-\text{O}^-$  stretching in highly depolymerized phosphate species. It is expected, therefore, that their Raman cross sections are similar, resulting in proportionality between area ratio and mole-fraction abundance ratio. The 1100 and 1150  $\text{cm}^{-1}$  bands, in contrast, are assigned to different vibrations in species that are structurally quite different ( $\text{Si}-\text{O}^-$  and  $\text{Si}-\text{O}^0$  stretching in  $\text{Q}^3$  and  $\text{Q}^4$  species, respectively). The Raman cross sections for those vibrations differ by a factor of 6–10 (MySEN 1995). Consequently, although  $A_{1100}/A_{1150}$  is positively correlated with the  $\text{Q}^3/\text{Q}^4$  abundance ratio, the two ratios are not proportional.

This change of phosphate complexing across the glass-transition temperature range requires interaction with the silicate solvent. Although there may be a small fraction of  $\text{Q}^2$  species present, the two principal species are of the  $\text{Q}^3$  and  $\text{Q}^4$  types, as evidenced in particular by the strong bands near 1100 and 1150  $\text{cm}^{-1}$ , respectively. The integrated intensity ratio of these two bands,  $A_{1100}/A_{1150}$ , increases across the glass-transition temperature range (Fig. 3B), which suggests that the change in phosphate speciation is also associated with a change in silicate polymerization. By using stoichiometric notations,  $\text{Si}_2\text{O}_5^{2-}$  and  $\text{SiO}_2$ , for the  $\text{Q}^3$  and  $\text{Q}^4$  species, a simple expression describes the equilibrium involving silicate and phosphate species:  $\text{P}_2\text{O}_7^{4-} + \text{Si}_2\text{O}_5^{2-} \leftrightarrow 2\text{PO}_4^{3-} + 2\text{SiO}_2$ . It follows from these observations that as the phosphate species undergo polymerization, O is exchanged between the phosphate and silicate species, so that the silicate melts actually become less polymerized as the phosphate polymerizes.

It is clear from the above considerations that when discussing phosphate-solution mechanisms in silicate melts, the quantitative evaluation of the interaction between silicate and phosphate requires determination of the phosphate speciation in the melt at relevant temperatures. By employing speciation data from glasses for this purpose, the effect of dissolved P on the polymerization of a silicate melt leads to an overestimation of the change in degree of polymerization.

#### ACKNOWLEDGMENTS

This research was partially supported by CIW-CNRS P.I.C.S. no. 142. Critical reviews by A. Hofmeister and R.J. Ryerson greatly improved the manuscript.

#### REFERENCES CITED

- Davidon, W.C. (1966) Variable metric method for minimization. ANL 5990 (3rd. rev.). Argonne National Laboratory.
- Dupree, R., Holland, D., and Mortua, M.G. (1988) The role of small amounts of  $\text{P}_2\text{O}_5$  in the structure of alkali silicate glasses. *Physics and Chemistry of Glasses*, 29, 18–21.
- Gan, H., and Hess, P.C. (1992) Phosphate speciation in potassium aluminosilicate glasses. *American Mineralogist*, 77, 495–506.
- Harrison, T.M., and Watson, E.B. (1984) The behavior of apatite during crustal anatexis: Equilibrium and kinetic considerations. *Geochimica et Cosmochimica Acta*, 48, 1467–1477.
- Kracek, F.C. (1930) The system sodium oxide-silica. *Journal of Physics and Chemistry of Solids*, 34, 1583–1598.
- Kushiro, I. (1975) On the nature of silicate melt and its significance in magma genesis: Regularities in the shift of liquidus boundaries involving olivine, pyroxene, and silica materials. *American Journal of Science*, 275, 411–431.
- London, D. (1987) Internal differentiation of rare earth-element pegmatites: Effects of boron, phosphorous, and fluorine. *Geochimica et Cosmochimica Acta*, 51, 403–420.
- McMillan, P.F., Wolf, G.H., and Poe, B.T. (1992) Vibrational spectroscopy of silicate liquids and glasses. *Chemical Geology*, 96, 351–366.
- MySEN, B.O. (1992) Iron and phosphorus in calcium silicate quenched melts. *Chemical Geology*, 98, 175–202.
- MySEN, B.O. (1995) Structural behavior of  $\text{Al}^{3+}$  in silicate melts: In-situ, high-temperature measurements as a function of bulk chemical composition. *Geochimica et Cosmochimica Acta*, 59, 455–474.
- MySEN, B.O. (1996) Haplodesitic melts at magmatic temperatures: In-situ, high-temperature structure and properties of melts along the join  $\text{K}_2\text{Si}_4\text{O}_9-\text{K}_2(\text{Al})_4\text{O}_6$  to 1236 °C at atmospheric pressure. *Geochimica et Cosmochimica Acta*, 60, 3665–3686.
- MySEN, B.O., and Frantz, J.D. (1992) Raman spectroscopy of silicate melts at magmatic temperatures:  $\text{Na}_2\text{O}-\text{SiO}_2$ ,  $\text{K}_2\text{O}-\text{SiO}_2$  and  $\text{Li}_2\text{O}-\text{SiO}_2$  binary compositions in the temperature range 25–1475 °C. *Chemical Geology*, 96, 321–332.
- (1993) Structure of silicate melts at high temperature: In-situ measurements in the system  $\text{BaO}-\text{SiO}_2$  to 1669 °C. *American Mineralogist*, 78, 699–709.
- MySEN, B.O., Ryerson, F.J., and Virgo, D. (1981) The structural role of phosphorous in silicate melts. *American Mineralogist*, 66, 106–117.
- MySEN, B.O., Virgo, D., and Seifert, F.A. (1982) The structure of silicate melts: Implications for chemical and physical properties of natural magma. *Reviews of Geophysics*, 20, 353–383.
- Nelson, C., and Tallant, D.R. (1984) Raman studies of sodium silicate glasses with low phosphate contents. *Physics and Chemistry of Glasses*, 25, 31–39.
- Pichavant, M., Montel, J.-M., and Richard, L.R. (1992) Apatite solubility in peraluminous liquids: Experimental data and an extension of the Harrison model. *Geochimica et Cosmochimica Acta*, 56, 3855–3861.
- Ryerson, F.J., and Hess, P.C. (1980) The role of  $\text{P}_2\text{O}_5$  in silicate melts. *Geochimica et Cosmochimica Acta*, 44, 611–625.
- Stebbins, J.F., Farnan, I., and Xue, X. (1992) The structure and dynamics of alkali silicate liquids: A view from NMR spectroscopy. *Chemical Geology*, 96, 371–386.
- Toplis, N.J., Libourel, G., and Carroll, M.R. (1994) The role of phosphorus in crystallization processes of basalt: An experimental study. *Geochimica et Cosmochimica Acta*, 58, 797–810.
- Watson, E.B. (1976) Two-liquid partition coefficients: Experimental data and geochemical implications. *Contributions to Mineralogy and Petrology*, 56, 119–134.
- Wolf, M.B., and London, D. (1994) Apatite dissolution into peraluminous haplogranitic melts: An experimental study of solubilities and mechanisms. *Geochimica et Cosmochimica Acta*, 58, 4127–4145.
- Wyllie, P.J., and Tuttle, O.F. (1964) Experimental investigation of silicate systems containing two volatile components: III. The effects of  $\text{SO}_2$ ,  $\text{P}_2\text{O}_5$ ,  $\text{HCl}$ , and  $\text{Li}_2\text{O}$  in addition to  $\text{H}_2\text{O}$  on the melting temperatures of albite and granite. *American Journal of Science*, 262, 930–939.

MANUSCRIPT RECEIVED JUNE 19, 1996

MANUSCRIPT ACCEPTED NOVEMBER 6, 1996